文章编号:1000-8055(2014)07-1598-08　　doi:10.13224/j.cnki.jasp.2014.07.012

Performance investigation of intercooler operating in wet condition using distributed parameter model

ZHOU Ya-feng[1,2], LIU Gui-lin[3], HAN Ya-hui[4], YANG Chun-xin[3], ZHU Zhi-li[1]

(1. School of Energy and Power Engineering, Beijing University of Aeronautics and Astronautics, Beijing 100191, China;
2. Shenyang Engine Design and Research Institute, Aviation Industry Corporation of China, Shenyang 110015, China;
3. School of Aeronautic Science and Engineering, Beijing University of Aeronautics and Astronautics, Beijing 100191, China;
4. Mechanical Engineering Department, Army Aviation Institute, the Chinese People's Liberation Army, Beijing 100123, China)

Abstract: The performance of a marine gas turbine intercooler operating in wet condition was evaluated. The intercooler was a cross-flow plate-fin heat exchanger that used air and pure water as its working fluids at the hot and cold sides, respectively. The heat transfer performance and the water vapor condensation were investigated for a relative humidity of the inlet air that reached 100% during warship cruise. The condensation of the water vapors increased the hot side outlet temperature by a certain amount, which could in turn influence the performance of the compressor downstream. The condensate film thickness and the void fraction were calculated based on an annular two-phase flow model. It is found that water vapor condensation in hot flow channel increases the outlet temperature with a maximum value of 7.3 ℃ in the case of 100% relative humidity. The calculated liquid film thickness reaches a maximum value of 4 μm, which indicates negligible thermal resistance to heat transfer. The results of liquid film thicknesses also provide a qualitative prediction of the diameter distribution of the condensate water droplets.

Key words: intercooler; wet condition; plate-fin heat exchanger; condensation; film thickness

CLC number: V231.1; TK172　　**Document code**: A

Nomenclature

A	Total heat transfer area at one side (m^2)
A_c	Minimum cross-sectional area at one side (m^2)
b	Partition distance at one side (mm)
D_e	Hydraulic diameter (mm)
s	Fin space (mm)
L	Flow length at one side (mm)
N	Number of layers at one side
β	Ratio of total transfer area of one side to volume between plates at that side
h	Fin thickness (mm)
δ	Liquid film thickness (μm)
σ	Ratio of fin area of one side to total transfer area at that side
$\dot{m}$	Mass flow rate of hot or cold fluids (kg/s)
I	Enthalpy of the working fluids (J/kg)
$\dot{m}_a$	Mass flow rate of dry air(kg/s)
$t_{in,h}$	Inlet temperature at hot side(℃)
$t_{ex,h}$	Outlet temperature at hot side(℃)
$\dot{m}_w$	Mass flow rate of cooling water(kg/s)
$t_{in,c}$	Inlet temperature at cold side(℃)
$t_{ex,c}$	Outlet temperature at cold side(℃)

Received:2014-01-07

In the past several decades, the marine gas turbine has been developed for its obvious advantages in marine propulsion systems and experienced many fuel efficient improvements, which are in line with aero-engine technology advances. High efficiency gas turbines have significant features in their intercooling and recuperating systems, which aim to improve the part-power cycle efficiency. In these systems, an intercooler is used to reduce the work required to drive the high pressure compressor but more importantly provides a low recuperator air side inlet temperature to permit maximum heat recovery in the recuperator[1]. These intercoolers are basically gas-to-liquid heat exchangers with different types of extended surfaces on the air-side to enhance the heat transfer rate at the larger thermal resistance side[2]. There are many extended surface concepts and heat exchanger types that can be used or are already used in intercoolers[3-5].

Saidi et al. compared several different types of intercoolers at the same heat duty and discovered that a plate-fin heat exchanger using a strip-fin or a triangular-cross-section plain-fin provide the smallest pressure drop and weight[6]. In the advanced cycle marine gas turbine WR-21, an offset strip-fin geometry was used as the heat transfer surface[7]. Most published literatures for the compact heat exchanger document its performance under dry conditions. Only a few published literatures focused on the performance of the fin-tube heat exchangers in a wet condition[8-12]. As far as the plate-fin heat exchangers are concerned, few studies have concentrated on their performance in a wet condition and have been reported to the authors' knowledge.

This paper mainly focuses on the heat transfer performance of a cross-flow plate-fin intercooler operating in a wet condition using a distributed parameter model. The working fluids are air and pure water in the hot and cold sides, respectively. The wet operating condition is assumed as 100% relative humidity at the sea surface. The main target of the current work is to investigate the influence of the existing water vapor or the condensate liquid on the heat transfer performance of the intercooler and to provide a qualitative prediction method for the entrained water droplets from the hot flow passages. The pressure decrease of both fluids is not investigated in the current work.

1 Profile of intercooler

The examined intercooler was a cross-flow compact heat exchanger assembled with a rectangular plain-fin and a triangular strip-fin based on the fin data published in Kay and London[13]. Detailed information for the structure of the intercooler is shown in Table 1. Tests of the intercooler were performed in six different cases, which cover the entire working conditions of the intercooler as shown in Table 2. These tests were only performed for dry operating conditions (dry air as hot working fluid) and can be used to verify the distributed parameter model described in the following section. For a wet operating condition, the amount of water vapor in the inlet air was calculated at 100% relative humidity of the wet air at the standard sea surface (25 ℃, 101.325 kPa) to examine the condensation characteristics of the intercooler.

Table 1 Design profile of intercooler

Parameter	Hot side (Plain-fin)	Cold side (Strip-fin)
b/mm	6.325	1.91
s/mm	2.13	1.31
h/mm	0.152	0.102
L/mm	480	420
N	51	52
$\beta/(m^2/m^3)$	1289	2490
D_e/mm	2.87	1.403
σ	0.769	0.611
A/m^2	77.738	46.236
A_c/m^2	0.1468	0.033

Table 2 Test results of intercooler for dry conditions

Parameter	Case					
	1	2	3	4	5	6
$\dot{m}_a$/(kg/s)	9.97	8.9	7.7	6.4	5.1	3.0
$t_{in,h}$/℃	167.4	158.0	147.3	132.5	109.8	64.5
$t_{ex,h}$/℃	38.6	37.0	35.4	32.7	29.7	24.0
$\dot{m}_w$/(kg/s)	16.4	16.4	16.4	16.4	16.4	16.4
$t_{in,c}$/℃	20.5	20.6	21.0	20.6	20.8	20.4
$t_{ex,c}$/℃	39.4	36.5	33.7	30.0	26.8	22.2

2 Mathematical model

2.1 Distributed parameter model (DPM)

The entire gas turbine intercooler was meshed into grids using a distributed parameter model that was first proposed by Zhang et al.[14-17]. This model features with a simplified meshing method, which uses the fin space at each side of a heat exchanger to split the whole exchanger into a group of fluid control volumes as shown in Fig. 1. The DPM meshing method significantly reduces the grid amount compared to CFD method so that the calculation time can be shortened abruptly.

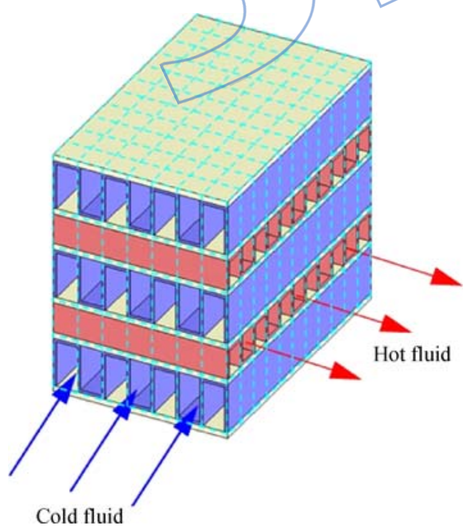

Fig. 1 Mesh of DPM

Additionally, the thermal properties of the working fluids can be localized at each control volume to guarantee the accuracy of the calculation compared to the CFD method. Interested readers should refer to the work of Zhang[16] for details regarding the DPM method.

Figure 2 displays the control volume of the partition wall. At a steady heat transfer condition, the heat balance for the current control volume can be constructed using the two neighboring fluid control volumes (volume 1 and volume 2 in Fig. 2) and the four adjacent wall control volumes (volume 3 to volume 6). The governing equation was described in detail in the work by Zhang[16]. For the working fluids control volume in Fig. 3, the heat balance equation was established between the working fluid control volume and its four adjacent wall elements[16].

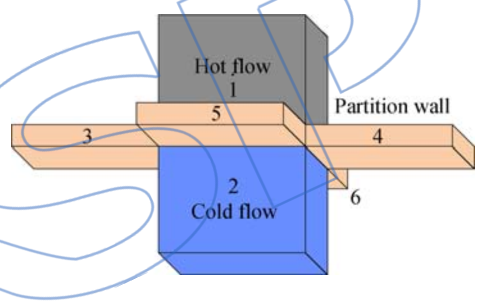

Fig. 2 Control volume of partition wall

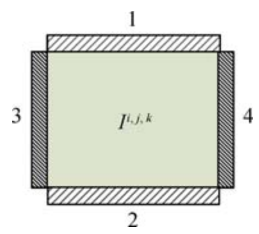

Fig. 3 Control volume of working fluids

When liquid water condenses in the control volume, the enthalpy of the working fluid is used to accommodate the liquid water heat transfer instead of temperature and can be calculated using the following expression:

$$I^{i,j,k} = c_{pa}^{i,j,k} \cdot t^{i,j,k} + d_v^{i,j,k}(I_{fg} + c_{pv} \cdot t^{i,j,k}) + d_l^{i,j,k} \cdot c_{pl}^{i,j,k} \cdot t^{i,j,k} \tag{1}$$

where c_{pa}, c_{pv}, and c_{pl} are the isobaric heat capacities of air, water vapor and liquid water, respectively (J/(kg·K)); d_v and d_l are the absolute humidity and the amount of water in the current control volume (kg/kg dry air); t is the fluid temperature in Celsius; superscript i, j, k

symbolizes the ith fluid layer, the jth flow channel and the kth control volume. c_{pv} is a constant value of 1 840 J/(kg·K), while the other two values are localized for each control volume.

By combining the governing equations on the partition wall and the fluid control volume with Eq. (1), the enthalpy distribution of the liquids in the hot and cold layers of the heat exchanger can be obtained. Thus, the fluid temperature distribution and the humidity distribution can be calculated afterwards.

2.2 Annular model for two-phase flow

During the operation in wet condition, humid air may condense as it flows in the gas turbine intercooler when the outlet temperature decreases to a value lower than that of the dew point. In an extreme case, the relative humidity over the sea surface during the warship cruise reaches 100%, and the amount of water in the humid air is 0.019 8 kg/kg dry air (25 ℃, 101.325 kPa). This amount of water is so small that the Re of the condensate liquid film would be far below 100, which may produce a very smooth annular flow in the flow passages (Fig. 4).

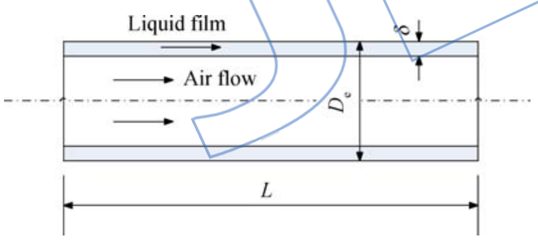

Fig. 4　Schematic of annular flow

Hence, the analytical solution for pure annular flow is adopted to calculate the void fraction and the condensate film thickness. The annular flow expressions are provided below[18]:

$$\Phi_{lo}^2 = \frac{1}{(1-\alpha)^2} \tag{2}$$

$$1-\alpha = \frac{4\delta}{D_e} \qquad \delta \ll D_e \tag{3}$$

where α is the void fraction, which is the ratio of the cross-sectional area of the air flow to the flow passage; δ is the liquid film thickness, and Φ_{lo} is the two-phase flow Lockhart-Martinelli factor when the liquid flows in the passages only.

3 Results and discussion

3.1 Operating in dry condition

Dry condition test results are obtained using the method proposed in Ref. [13] and are used to verify the DPM method. The test results are shown in Table 2, and are compared with the results calculated by the DPM method as shown in Fig. 5. It is shown that the outlet fluid temperature obtained by tests ($t_{ex,test}$) agreed with the value calculated by DPM method ($t_{ex,dpm}$) very well (within ±95% accuracy), which indicates that the DPM method is feasible for the calculation of a compact heat exchanger.

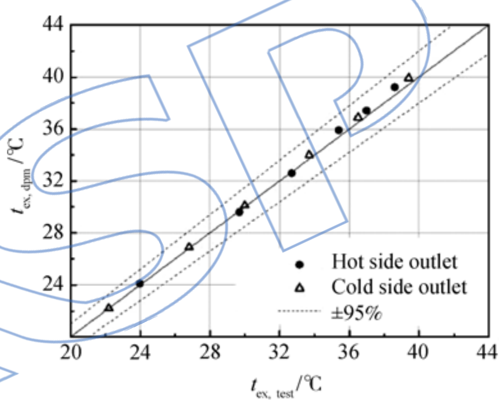

Fig. 5　Comparison of outlet temperature from experiments and DPM method

Figure 6 to Fig. 8 demonstrate the temperature distribution in hot layer (t_h), cold layer (t_c) and the partition wall (t_w) in dry condition. The x-axis represents the flow passage number in which the cold fluid flows into the intercooler, and the y-axis represents that at hot fluid side. The convective heat transfer coefficient at the cold side (water side) is much higher than that of the hot side (air side), which enables a quick heat transfer from the partition wall to the cold fluid. Thus, the temperature distribution in the partition wall and the cold layer looks similar as shown in the comparison between Fig. 7 and Fig. 8. These results strongly prove that the DPM method provides a precise description of the fluid temperature behavior. In the following section, an intercooler operating in wet condition is investigated using the DPM method.

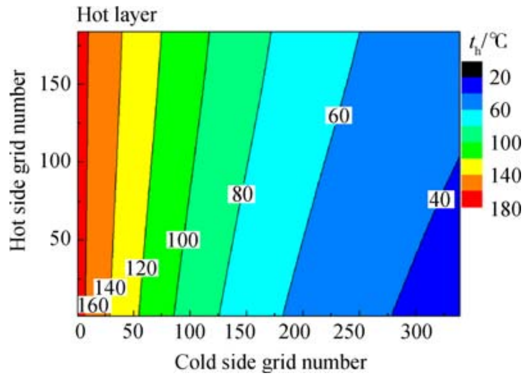

Fig. 6 Temperature distribution of hot layer in dry condition

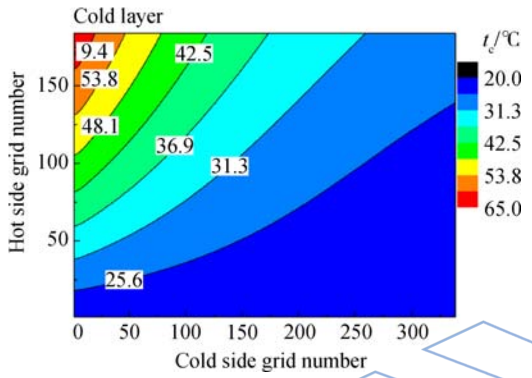

Fig. 7 Temperature distribution of cold layer in dry condition

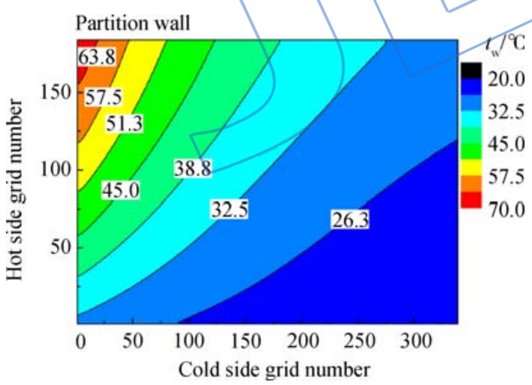

Fig. 8 Temperature distribution of partition wall in dry condition

3.2 Operating in wet condition

When the gas turbine intercooler operates in a condition that the air humidity at the sea surface reaches 100%, liquid water condensation may occur in the hot flow passages for the temperature of the partition wall could be lower than the dew point temperature of the hot fluid. The condensation effect must be examined in detail because it may affect the temperature distribution in the partition wall and cause the hot fluid outlet temperature to increase by a certain amount. Generally, a high-pressure compressor is directly installed after the intercooler, and a certain increase in the fluid temperature at the outlet of the intercooler may cause the compressor efficiency to decrease.

To investigate the intercooler performance in wet condition, humid air with 100% relative humidity based on the sea level condition was considered as the working fluid in the hot side. The study was based on the operating condition in case 1.0. As seen from the comparison between Fig. 6 and Fig. 9, the hot fluid temperature in wet condition is higher than that in dry condition. The outlet temperature of the hot fluid in wet condition is 45.9℃ for case 1.0, which is 7.3℃ higher than that of dry condition (Table 2). The increase in the outlet temperature encompasses 5.7% of the temperature difference between the inlet and outlet at the hot side in dry condition and can be attributed to the increase in the wall temperature caused by water vapor condensation.

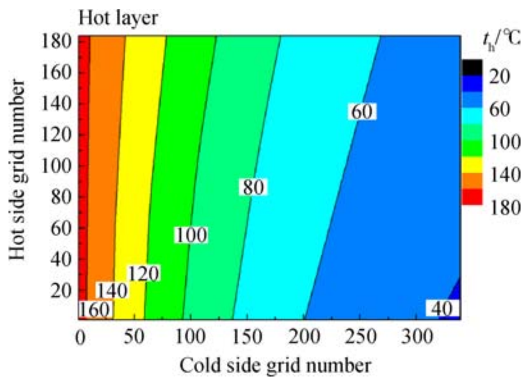

Fig. 9 Temperature distribution of hot layer in wet condition

Figure 10 and Fig. 11 show the temperature distribution in the cold layers and on the partition walls. By comparison of Fig. 7 and Fig. 8 respectively, it is obviously shown that the temperatures of cold fluid and the partition wall are slightly higher than that in dry operating condition. These results are caused by the liquid condensation on the partition wall. The latent heat released from the condensate increased the wall temperature and cold fluid temperature by 2 to 10 ℃, which in turn decreased the heat transfer between hot fluid and the partition wall, so that the hot fluid temperature increased a certain amount.

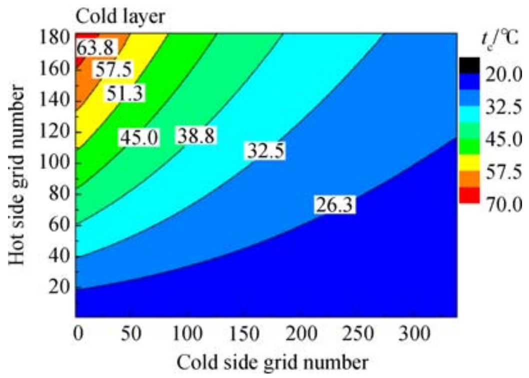

Fig. 10　Temperature distribution of cold layer in wet condition

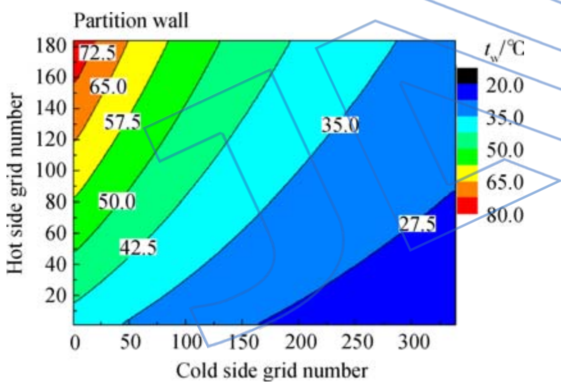

Fig. 11　Temperature distribution of partition wall in wet condition

Figure 12 demonstrates the water condensation D_l in hot layers. As can be seen, the condensation occurred in more than half the area of hot layer. The amount of condensation increased gradually towards the end of the flow passages (hot fluid flows from left to right), especially in the area that is close to the inlet of cold fluid (cold fluid flows from bottom to top). This area corresponds with the flow region where the wall temperatures are lower than the dew point temperature of hot fluid.

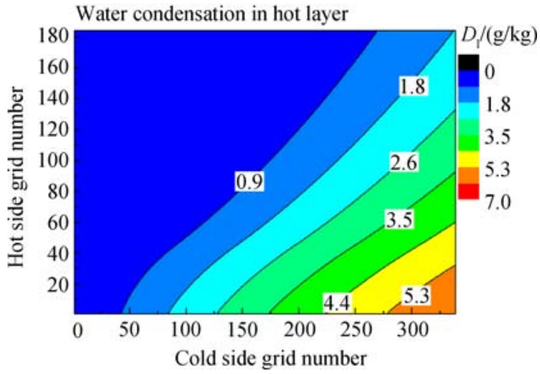

Fig. 12　Condensate distribution

The accumulation of liquid water in the hot flow passages may provide entrained droplets that risk the operation safety of the compressor installed downstream. To account for the droplets' characteristics, the liquid film thickness must be understood to provide a rough prediction of the droplets' diameter.

A pure annular flow model was combined with the DPM method to calculate the liquid film thickness in the hot flow passages. This calculation does not consider the temporal cumulative effect of the liquid water. The liquid film thickness distribution as shown in Fig. 13 only represents the steady state results. The liquid film thickness has a magnitude of only microns, which is quite small compared with the hydraulic diameter of the hot flow passages.

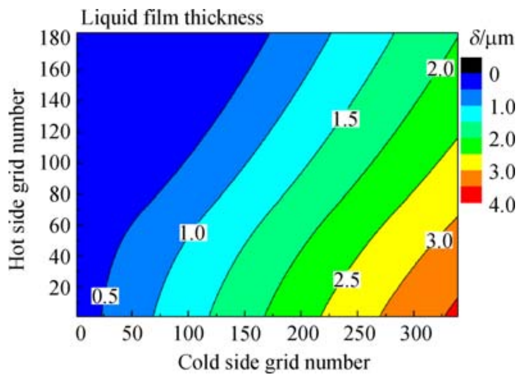

Fig. 13　Liquid film thickness distribution

Figure 14 shows the void fraction results in one of the hot layers. The results are in good accordance with the liquid film thickness distribution in Fig. 13. In addition, the void fraction results indicate that the amount of liquid water occupies very little space in the flow passages and could even be neglected with respect to the film thickness. According to the liquid film thickness, the thermal resistance in the liquid film is negligible comparing to the convective thermal resistance. Thus, the temperature of liquid film was assumed to be equal to the wall temperature.

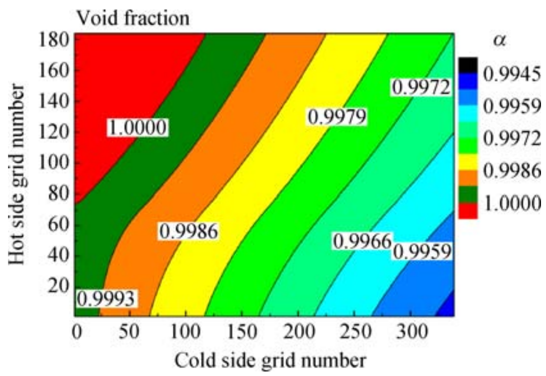

Fig. 14 Void fraction result

As the liquid film flows to the end of the passages, the liquid film thickness increases gradually due to the accumulation effect and droplets entrainment may occur. For the entrained droplets, the diameter is larger than the liquid film thickness if the temporal liquid accumulation is considered. Because no experimental studies are published to validate the current results, this study provides a qualitative prediction for the droplets' diameter. A quantitative prediction may require a precise description of the liquid accumulation effect in the time domain, and further study will be necessary.

4 Conclusions

This paper studies the performance of a gas turbine intercooler operating in wet condition using a distributed parameter model. The DPM method significantly reduces the grid amount but maintains comparable accuracy during the calculation of the intercooler compared to the CFD method. Dry condition test results validate the feasibility of the DPM method. A pure annular flow model was applied with the DPM method to study the condensation effect in the hot flow passages of the intercooler. The following results can be concluded:

1) Water vapor condensation increases the outlet temperature of the hot fluid by a certain amount. In the case of 100% relative humidity, water vapor condensation decreases the temperature difference between the inlet and outlet at the hot side in dry condition by 5.7% (7.3 ℃). This result may cause the efficiency of the compressor installed behind the intercooler to decrease and may reduce the performance of the whole gas turbine system.

2) Condensation occurs in more than half the area of the hot layer. The amount of water condensate increases along the flow passages, especially in the area close to the inlet of the cold side. The of the resulting liquid film thickness corresponds to the amount of condensate and reaches a maximum value of 4.0 μm.

3) The void fraction results indicate that the amount of liquid water that condenses in the hot flow passages encompasses only a small number of the cross-sectional areas and could be neglected with respect to its thermal resistance.

Further experimental study to investigate the condensed liquid film thickness should be performed to validate the results presented in the current work quantitatively and to address the problem of the entrained droplets' diameter in the flow passages.

References:

[1] Parker M L, MacLeod P K, Coulson M. Advances in a gas turbine system for ship propulsion[R]. Lisbon, Portugal: RTO AVT Symposium on Gas Turbine Engine Combustion, Emissions and Alternative Fuels, 1998.

[2] Saidi A, Sunden B, Eriksson D. Intercoolers in gas turbine systems and combi-processes for production of electricity [R]. ASME Paper 2000-GT-234, 2000.

[3] Webb R L. Principles of enhanced heat transfer[M]. New York, USA: John Wiley and Sons, 1994.

[4] Sunden B, Heggs P J. Recent advances in analysis of heat transfer for fin type surfaces[M]. [S. l.]: WIT Press, 2000.

[5] Kraus A D, Aziz A, Welty J. Extended surface heat transfer[M]. New York, USA: John Wiley and Sons, 2001.

[6] Saidi A, Eriksson D, Sunden B. Analysis of some heat exchanger concepts for use as gas turbine intercoolers[J]. International Journal of Heat Exchangers, 2002, 3(2): 241-260.

[7] Crisalli A J, Parker M L. Overview of the WR-21 intercooled recuperated gas turbine engine for a modern fleet [R]. ASME Paper 93-GT-231, 1993.

[8] Bougrious C, Bessaih R, Bontemps A. Experimental study of performances of industrial heat exchangers functioning in wet regime[J]. Interational Journal of Heat Exchanger, 2005, 6(2): 179-202.

[9] Zhang Y M, Ding G L, Ma X K. Comparison of air-side characteristics of wavy fin-and-tube heat exchangers under dry and wet conditions[J]. Chinese Journal of Mechanical Engineering, 2008, 44 (9): 209-214.

[10] Yun R, Kim Y B, Kim Y C. Air side heat transfer characteristics of plate finned tube heat exchangers with slit fin configuration under wet conditions[J]. Applied Thermal Engineering, 2009, 29(14/15): 3014-3020.

[11] Park Y G, Jacobi A M. Asimple air-side data analysis method for partially wet flat-tube heat exchangers[J]. Heat Transfer Engineering, 2011, 32 (2): 133-140.

[12] Phan T L, Chang K S, Kwon Y C et al. Experimental study on heat and mass transfer characteristics of louvered fin-tube heat exchangers under wet condition[J]. International Communications in Heat and Mass Transfer, 2011, 38(7): 893-899.

[13] Kay W M, London A L. Compact heat exchangers[M]. 3rd ed. New York: McGraw-Hill, 1984.

[14] Zhang L N, Yang C X. Heat transfer and thermodynamic analysis of internal flow based on distributed parameter model[J]. Journal of Chemical Industry and Engineering, 2008, 59(12): 2978-2984. (in Chinese)

[15] Zhang L N, Yang C X. Optimization of compact heat exchanger based on 3D distributed parameter model[J]. Journal of Aerospace Power, 2008, 23(4): 617-622. (in Chinese)

[16] Zhang L N. Design and optimization of heat exchanger based on distributed parameter model[D]. Beijing: Beijing University of Aeronautics and Astronautics, 2008. (in Chinese)

[17] Zhang L N, Yang C X, Zhou J H. A distributed parameter model and its application in optimizing the plate-fin heat exchanger based on the minimum entropy generation[J]. International Journal of Thermal Sciences, 2010, 49(8): 1427-1436.

[18] Xu J Y. Boiling heat transfer and two-phase flow[M]. 2nd ed. Beijing: Atomic Energy Press, 2001. (in Chinese)